UC Berkeley
UC Berkeley Previously Published Works

Title
Anisotropic Ion Diffusion and Electrochemically Driven Transport in Nanostructured Block Copolymer Electrolytes

Permalink
https://escholarship.org/uc/item/2gp7q4gm

Journal
The Journal of Physical Chemistry B, 122(4)

ISSN
1520-6106

Authors
Timachova, Ksenia
Villaluenga, Irune
Cirrincione, Lisa
et al.

Publication Date
2018-02-01

DOI
10.1021/acs.jpcb.7b11371

Peer reviewed

eScholarship.org Powered by the California Digital Library
University of California

THE JOURNAL OF PHYSICAL CHEMISTRY B

Article

Cite This: J. Phys. Chem. B 2018, 122, 1537−1544

pubs.acs.org/JPCB

Anisotropic Ion Diffusion and Electrochemically Driven Transport in Nanostructured Block Copolymer Electrolytes

Ksenia Timachova,[#,†,‡] Irune Villaluenga,[#,†,‡] Lisa Cirrincione,[§] Mallory Gobet,[§] Rajashree Bhattacharya,[†] Xi Jiang,[‡] John Newman,[†] Louis A. Madsen,[∥] Steven G. Greenbaum,[*,§] and Nitash P. Balsara[*,†,‡]

[†]Department of Chemical and Biomolecular Engineering, University of California, Berkeley, Berkeley, California, United States

[‡]Materials Sciences Division, Lawrence Berkeley National Laboratory, Berkeley, California, United States

[§]Department of Physics and Astronomy, Hunter College, City University of New York, New York, New York, United States

[∥]Department of Chemistry, Virginia Polytechnic Institute and State University, Blacksburg, Virginia, United States

ABSTRACT: Nanostructured block copolymer electrolytes have the potential to enable solid-state batteries with lithium metal anodes. We present complete continuum characterization of ion transport in a lamellar polystyrene-*b*-poly(ethylene oxide) copolymer/lithium bis(trifluoromethanesulfonyl)imide (LiTFSI) electrolyte as a function of salt concentration. Electrochemical measurements are used to determine the Stefan−Maxwell salt diffusion coefficients $\mathcal{D}_{+,0}$, $\mathcal{D}_{-,0}$, and $\mathcal{D}_{+,-}$. Individual self-diffusion coefficients of the lithium- and TFSI-containing species were measured by pulsed-field gradient NMR (PFG-NMR). The NMR data indicate that salt diffusion is locally anisotropic, and this enables determination of a diffusion coefficient parallel to the lamellae, $D_{\parallel}$, and a diffusion coefficient through defects in the lamellae, $D_{\perp}$. We quantify anisotropic diffusion by defining an NMR morphology factor and demonstrate that it is correlated to defect density seen by transmission electron microscopy. We find agreement between the electrochemically determined Stefan−Maxwell diffusion coefficients and the diffusion coefficient $D_{\perp}$ determined by PFG-NMR. Our work indicates that the performance of nanostructured block copolymer electrolytes in batteries is strongly influenced by ion transport through defects.

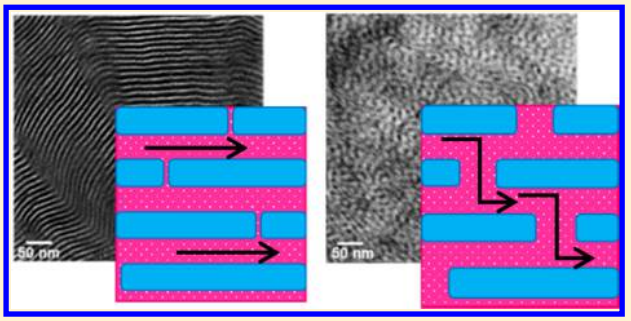

INTRODUCTION

Nanostructured block copolymers doped with lithium salts are promising candidates for use as electrolytes in solid-state lithium batteries. They have the potential to enable lithium metal anodes by providing ion conduction, stability to lithium, and mechanical rigidity against dendrites.[1] Complete continuum characterization of transport in electrolytes requires knowledge of three parameters: conductivity, the salt diffusion coefficient, and the transference number.[2] Methods for measuring these parameters are available in the literature,[3−5] but they have not yet been applied to block copolymer electrolytes despite the large body of work on characterization of ion transport in these systems.[6−19]

Nanostructured block copolymers form ordered phases where coherent order is restricted to regions referred to as grains. In Figure 1, we show a schematic of a lamellar grain composed of a polystyrene-*b*-poly(ethylene oxide) (SEO) copolymer with added salt. Ion transport occurs predominantly in the conducting poly(ethylene oxide)-rich phase in the x and y dimensions along the plane of the lamellae. We expect salt diffusion in the x−y plane, $D_{\parallel}$, parallel to the lamellae to be significantly higher than that along the z direction, $D_{\perp}$, perpendicular to the lamellae. Typically, block copolymer electrolytes are composed of a large collection of randomly oriented grains. Thus their continuum properties are isotropic; they only reflect local anisotropic transport indirectly.[7,8]

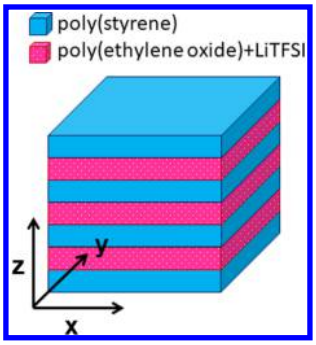

Figure 1. Single grain of SEO showing poly(ethylene oxide)+salt and poly(styrene) domains assembled into lamellae. The coordinate axes show the orientation of anisotropic diffusion vectors with diffusion through lamellae on the x and y axes and diffusion across lamellae in z.

A technique that has gained popularity for studying ion transport is pulsed-field gradient NMR (PFG-NMR), which allows for the direct measurement of the self-diffusion coefficients of ion species.[20−23] If the diffusion is locally anisotropic,

Received: November 17, 2017
Revised: December 20, 2017
Published: January 22, 2018

ACS Publications © 2018 American Chemical Society

DOI: 10.1021/acs.jpcb.7b11371
J. Phys. Chem. B 2018, 122, 1537−1544

then the displacement of ions is a function of the orientation of each grain with respect to the magnetic field gradient axis of the measurement. In this case, the signal attenuation does not follow a single exponential decay. This effect of anisotropy on transport has been studied in nanostructured polymeric and inorganic materials.[24−29]

In this work, we present the first complete set of continuum transport properties in a block copolymer electrolyte. We also present measurements of the anisotropic self-diffusion coefficients of the cations and anions using PFG-NMR. We use concentrated solution theory[2] to determine Stefan−Maxwell diffusion coefficients from the continuum measurements. We compare the self-diffusion coefficients and Stefan−Maxwell diffusivities.

METHODS

Materials. Anhydrous tetrahydrofuran (THF) and benzene were purchased from Sigma-Aldrich, lithium bis(trifluoromethanesulfonyl)imide, $Li[N(SO_2CF_3)_2]$ (LiTFSI), was purchased from Novolyte, and 5 kg/mol poly(ethylene oxide) (PEO(5)) was purchased from Polymer Source. The polystyrene-*b*-poly(ethylene oxide) copolymer with 16 kg/mol of each block (SEO(16−16)) was synthesized by sequential anionic polymerization of styrene, followed by ethylene oxide using methods described previously.[7]

LiTFSI was dissolved in anhydrous THF and added to solutions of SEO(16−16) in anhydrous benzene. For ease of lyophilization, the concentration of the LiTFSI−THF stock solution was adjusted so that the final solutions contained <5 vol % THF. SEO solutions were lyophilized without exposure to air for 1 week. Electrolytes were prepared at different LiTFSI salt concentrations (r = [Li]/[EO] = 0.03, 0.06, 0.12, 0.18, 0.24, and 0.3). SEO solutions were dried under vacuum at 90 °C for 24 h to remove trace solvents. Homopolymer 5 kg/mol poly(ethylene oxide) (PEO(5)/LiTFSI) electrolytes were used as a comparison and prepared as described previously.[5]

The characteristics of these electrolytes—the molar ratio of lithium atoms to ethylene oxide (EO) monomers, r, salt concentration, c, the molality, m, volume fraction of the conducting phase, ϕ_c, and EO solvent concentration, c_0—are summarized in Table 1. The salt concentration, c, and solvent concentration, c_0, were calculated according to

Table 1. Electrolyte Characteristics

	r	c (mol/cm^3)	c_0 (mol/cm^3)	m (mol/kg)	ϕ_c
SEO(16−16)	0.03	0.00070	0.02345	0.68	0.50
	0.06	0.00230	0.02162	1.36	0.52
	0.12	0.00224	0.01871	2.72	0.56
	0.28	0.00297	0.01649	4.09	0.59
	0.24	0.00354	0.01474	5.45	0.61
	0.30	0.00400	0.01332	6.81	0.64
PEO(5)	0.06	0.00230	0.02162	1.36	N/A

$$c = \frac{r}{r\frac{M_{LiTFSI}}{\rho_{LiTFSI}} + \frac{M_{EO}}{\rho_{EO}}}, \qquad c_0 = \frac{1}{r\frac{M_{LiTFSI}}{\rho_{LiTFSI}} + \frac{M_{EO}}{\rho_{EO}}}\left[\frac{\text{mol}}{\text{cm}^3}\right] \tag{1}$$

where M_{LiTFSI} = 287.09 g/mol is the molar mass of LiTFSI and M_{EO} = 44.05 g/mol is the molar mass of an ethylene oxide monomer. The densities of PEO/LiTFSI mixtures at 90 °C were measured as a function of r.[5] The density of pure poly(ethylene oxide) (r = 0) is ρ_{EO} = 1.128 g/cm^3. The measured densities of the mixtures were used to calculate the effective density of LiTFSI in PEO/LiTFSI, ρ_{LiTFSI} = 2.392 g/cm^3. We assume that all nonidealities of mixing are due to changes in the partial molar volume of LiTFSI.

The molality of the electrolyte, m, moles of LiTFSI salt per kilogram of PEO, is calculated according to

$$m = \frac{r}{M_{EO}} \cdot 1000\left[\frac{\text{mol}}{\text{kg}}\right] \tag{2}$$

The volume fraction of the conducting phase, ϕ_c, was calculated according to

$$\phi_c = \frac{\frac{M_{EO}}{\rho_{EO}} + \frac{rM_{LiTFSI}}{\rho_{LiTFSI}}}{\frac{M_{EO}}{\rho_{EO}} + \frac{rM_{LiTFSI}}{\rho_{LiTFSI}} + \frac{M_{PS}M_{EO}}{M_{PEO}\rho_{PS}}} \tag{3}$$

ρ_{PS} = 1.028 g/cm^3 is the density of polystyrene and M_{PEO} = 16 000 g/mol and M_{PS} = 16 000 g/mol are the molar masses of the poly(ethylene oxide) block and polystyrene block, respectively.

Electrochemical Characterization. All sample preparation was performed inside an argon glovebox (MBraun) to maintain water and oxygen levels below 1 and 5 ppm, respectively. Samples for conductivity measurements were prepared by heat-pressing the polymer at 130 °C into a 150 μm thick fiberglass−epoxy annular spacer (Garolite-10). The diameter of the electrolyte was taken to be the size of the hole in the annulus, 3.175 mm. High-purity aluminum foils, 17.5 μm thick, were pressed onto either side of the polymer as electrodes, and aluminum tabs (MTI Corporation) were attached to the electrodes with polyimide tape. The sample assembly was vacuum-sealed in an airtight aluminum-reinforced polypropylene pouch with tabs protruding out so the sample could be electrically probed. The thickness of the polymer sample was measured after conductivity measurements were performed using a precision micrometer. Impedance spectroscopy measurements were performed using a VMP3 potentiostat (Bio-Logic) with an ac amplitude of 20 mV in the frequency range 1 MHz−1 Hz. Impedance spectra were recorded at 10 °C intervals during heating and cooling scans between 30 and 130 °C. The ionic conductivity of the conducting phase in polymer electrolytes, σ, is calculated from the measured sample thickness, l, the cross-sectional area of the spacer, S, and electrolyte resistance, R_{el}, which was determined by methods discussed in literature.[30] The conductivity is given by

$$\sigma = \frac{l}{S^*R_{el}} \tag{4}$$

Lithium symmetric cells were prepared for steady-state current and restricted diffusion measurements of the electrolytes. Samples were made by pressing the polymer electrolyte into a Garolite-10 spacer and annealed at 130 °C for 3 h. After that, the electrolytes were sandwiched between two 150 μm lithium metal chips. Nickel tabs were secured to the lithium chips to serve as electrical contacts. The assembly was vacuum-sealed in a laminated aluminum pouch material (Showa-Denko) before removal from the glovebox. All samples were annealed at 90 °C for 2 h prior to electrochemical characterization.

Steady-state current and restricted diffusion measurements were performed using a Biologic VMP3 potentiostat. All measurements were performed at 90 °C. At the beginning of the experiment, cells were conditioned for three charge/discharge cycles at a low current density of 0.06 mA/cm^2. Each conditioning cycle

DOI: 10.1021/acs.jpcb.7b11371
J. Phys. Chem. B 2018, 122, 1537−1544

consisted of 4 h of charge, followed by 4 h of rest and 4 h of discharge. ac impedance spectroscopy was performed prior to potentiostatic polarization. Complex impedance measurements were acquired for a frequency range of 1 MHz to 1 Hz at an amplitude of 40 mV. The cell resistances were measured as a function of time by performing ac impedance spectroscopy every 10 min during polarization. Here the center of the ac input signal was offset by ΔV, and the amplitude was set to 20 mV to minimize disturbance of the polarization signal.

The steady-state transference number was determined from the relation[31]

$$t_{+,SS} = \frac{i_{SS}(\Delta V - i_{\Omega}R_{i,0})}{i_{\Omega}(\Delta V - i_{SS}R_{i,SS})} \tag{5}$$

where ΔV is the applied potential, i_{SS} is the current measured at steady-state, and $R_{i,0}$ and $R_{i,SS}$ are the initial and steady-state resistances of the interface, respectively. i_{Ω} is the initial current calculated according to the equation

$$i_{\Omega} = \frac{\Delta V}{R_{i,0} + R_{b,0}} \tag{6}$$

where $R_{i,0}$ and $R_{b,0}$ are cell resistances measured by ac impedance spectroscopy prior to polarization. If $R_{i,0} = R_{i,SS}$, that is, the interfacial impedance is independent of time, then eq 5 reduces to

$$t_{+} = \frac{i_{SS}R_{b,0}}{\Delta V - i_{SS}R_{i,0}} \tag{7}$$

first derived by Watanabe et al.[32]

Restricted diffusion measurements were performed using the polarization induced by the steady-state current experiment. The applied current was removed, and the cells were allowed to relax for up to 7 h while the open-circuit voltage, U, was measured at time intervals of 1 s. In the simple case where the $U(t)$ is a single exponential, the data are fit to the functional form

$$U(t) = k_0 + ae^{-bt} \tag{8}$$

where a and b are the fit parameters and k_0 is an empirically determined offset voltage. We posit that offset voltage, k_0, arises from small differences in the polymer/lithium interfaces in the symmetric cells. The offset voltage is much smaller than U over most of the experimental window.

The mutual salt diffusion coefficient, D_m, is calculated using

$$D_m = \frac{L^2 b}{\pi^2} \tag{9}$$

where b is from the fit of eq 8 and L is the thickness of the electrolyte. In our experiment $L \approx 100$ μm. The lower limits of the fits are such that $D_m t/L^2 > 0.05$.

Concentration cells were prepared using a similar cell configuration as previously described.[5] SEO/LiTFSI electrolytes were contained within a Garolite-10 spacer and were annealed at 130 °C for 3 h. A channel ~2.5 cm long and 0.4 cm wide was cut in the Garolite-10 spacer. Half of the channel was filled with reference electrolyte ($r = 0.03$), and the other half was filled with electrolytes at various r values. Lithium metal electrodes were placed on either end of the channel. Nickel tabs were secured to lithium metal electrodes, and assembly was vacuum-sealed in a laminated aluminum pouch material. Two or three concentration cells were prepared for each salt concentration. The open-circuit voltage, U, was measured for each cell at 90 °C using a Biologic VMP3 potentiostat.

Pulsed-Field Gradient NMR. All NMR samples were packed into 5 mm tubes in an argon-filled glovebox, and the tubes were then flame-sealed. Pulsed-field gradient NMR experiments were performed at 90 °C with a 7.05 T Varian-S Direct Drive Wide Bore spectrometer equipped with a DOTY Scientific PFG probe (DS-1034, 1400 G/cm maximum gradient). Single peaks were observed for ^{7}Li and ^{19}F at 287.0 and 117.1 MHz, respectively, corresponding to all lithium- and fluorine-containing species. A PFG-stimulated echo pulse sequence with one orthogonal spoiler gradient pulse and 5 ms longitudinal eddy current delay was used. Gradient pulse durations δ of 3 to 5 ms and diffusion delays Δ of 35 to 600 ms were used. The gradient strength g was linearly increased with 32 values steps from 2 up to 1100 G/cm as needed.

In a locally anisotropic nanostructured system, diffusion in a single grain oriented along one of the principal directions is described by the tensor

$$\boldsymbol{D} = \begin{bmatrix} D_{XX} & 0 & 0 \\ 0 & D_{YY} & 0 \\ 0 & 0 & D_{ZZ} \end{bmatrix} \tag{10}$$

For lamellae pictured in Figure 1, $D_{XX} = D_{YY} = D_{\parallel}$ and $D_{ZZ} = D_{\perp}$. For cylinders oriented along x, $D_{XX} = D_{\parallel}$ and $D_{ZZ} = D_{YY} = D_{\perp}$.

In a locally anisotropic lamellar nanostructured system, a stimulated echo PFG-NMR signal attenuation would follow the expression[33]

$$I = I_0 \frac{1}{2} \int_0^{\pi} \exp\left(-\gamma^2\delta^2 g^2\left(\Delta - \frac{\delta}{3}\right)(D_{\perp}\cos^2\theta + D_{\parallel}\sin^2\theta)\right)\sin\theta\, d\theta \tag{11}$$

where I is the signal intensity, γ is the gyromagnetic ratio, δ is the gradient pulse length, g is the gradient pulse strength, $D_{\parallel}$ is the diffusion coefficient along the conducting domains, $D_{\perp}$ is the diffusion coefficient orthogonal to the conducting domains, and θ is the angle between the z axis of the conducting domains shown in Figure 1 and the gradient field axis. The signal attenuation was fit to eq 11, subject to the additional constraint $D_{\parallel} > D_{\perp}$, using a nonlinear least-squares algorithm. T1 relaxation of all samples was measured to select appropriate diffusion and relaxation delay times. Each salt concentration was measured at a few different diffusion times, Δ, to probe a range of length scales in the nanostructure. We expect the same approach to apply to block copolymers comprising either lamellae or cylinders as the conducting domains.

While we focus on lamellar SEO/LiTFSI mixtures, we include previously published data from a PEO/LiTFSI electrolytes to demonstrate differences between homopolymer and block copolymer electrolytes. For homopolymer elecrolytes with isotropic diffusion, $D = D_{\parallel} = D_{\perp}$, and eq 11 reduces to a single exponential[34]

$$I = I_0 \exp\left(-D\gamma^2\delta^2 g^2\left(\Delta - \frac{\delta}{3}\right)\right) \tag{12}$$

Transmission Electron Microscopy. Transmission electron microscopy samples were prepared by cryo-microtoming 120 nm thick slices of SEO(16–16) annealed at 130 °C for 24 h and transferring to a lacey carbon-coated copper grid. The samples were then stained with ruthenium tetroxide vapor for 10 min.

DOI: 10.1021/acs.jpcb.7b11371
J. Phys. Chem. B 2018, 122, 1537–1544

Images were obtained on a Tecnai F20 (FEI Company) high-angle annular dark field scanning transmission electron microscope (HAADF-STEM) at a 200 kV.

RESULTS AND DISCUSSION

Electrochemical Characterization. In Figure 2, we show potential relaxation curves obtained in homopolymer 5 kg/mol

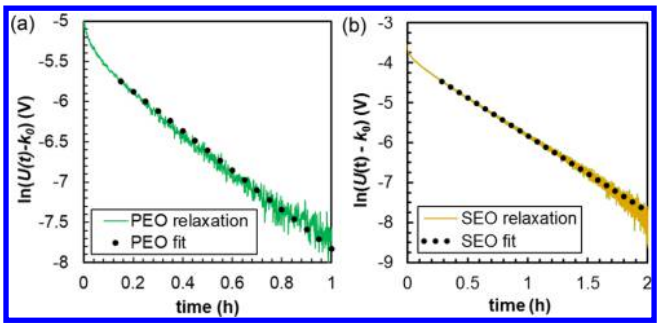

Figure 2. Plot of $\ln(U - k_0)$ versus t for (a) PEO(5)/LiTFSI at $r = 0.06$ and (b) SEO(16−16)/LiTFSI at $r = 0.18$. The experimental data are show as a line, and the fits are shown as black circles.

poly(ethylene oxide) electrolytes (PEO(5)/LiTFSI) and in polystyrene-*b*-poly(ethylene oxide) electrolytes SEO(16−16)/LiTFSI after stopping polarization in the restricted diffusion experiments. In both cases, the time dependence of the potential $U(t)$ follows single-exponential behavior; the plot of $\ln(U - k_0)$ versus time is linear. The fits of the data in Figure 2 to eqs 8 and 9 give the mutual salt diffusion coefficient, D_m. It is clear that the restricted diffusion experiments are consistent with a single diffusion coefficient.

D_m obtained using restricted diffusion is plotted as a function of salt concentration, r, in Figure 3a. The dependence of

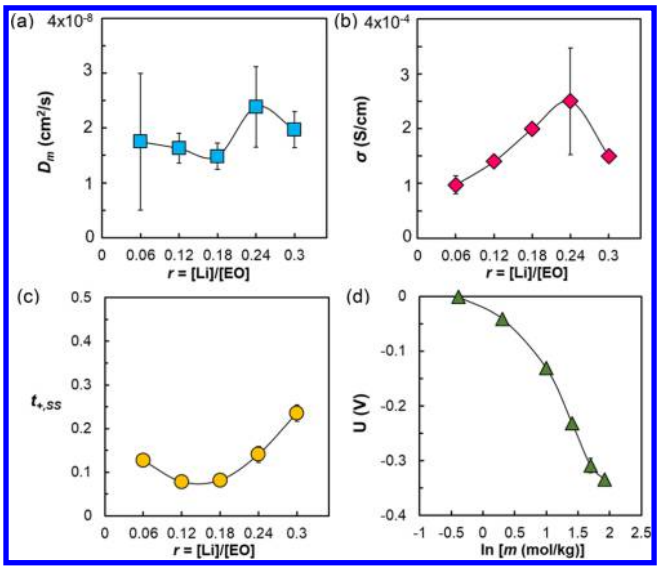

Figure 3. (a) Mutual diffusion coefficient, D_m, (b) ac conductivity, σ, (c) the steady-state current transference number, $t_{+,SS}$, as a function of salt concentration, r, and (d) the concentration potential in SEO(16−16) as a function of molality, m, at 90 °C.

D_m on r appears to be complex, showing a local minimum at $r = 0.18$ and local maximum at $r = 0.24$. The range of measured D_m values, however, is quite narrow, falling between (1.5 and 2.4) × 10^{-8} cm^2/s and is in agreement with the lower range of the distribution of diffusion values measured in SEO(16−16) reported previously.[8] Ionic conductivity, σ, measured using ac impedance, is plotted as a function of salt concentration, r, in Figure 3b. Figure 3b indicates that σ has a nonmonotonic dependence on r, reaching a maximum of 3×10^{-4} S/cm at $r = 0.24$, in agreement with previously published work.[6] The steady-state transference number, $t_{+,SS}$, is plotted as a function of salt concentration, r, in Figure 3c. The dependence of $t_{+,SS}$ on r is also nonmonotonic with a local minimum around $r = 0.12$. The potential difference between SEO(16−16)/LiTFSI electrolyte at a given salt concentration relative to the electrolyte at $r = 0.03$ ($m = 0.68$), U, is shown as a function of molality m in Figure 3d. The negative values reflect the lower potential of electrolytes with higher salt concentrations. The shape of U versus ln m is similar to that in homogeneous PEO/LiTFSI and PEO/NaTFSI electrolytes.[3,5]

The cation transference number derived from concentrated solution theory, t_+, can be calculated using the expression

$$t_+ = 1 + \left(\frac{1}{t_{+,SS}} - 1\right)\frac{(z_+\nu_+)FDc\phi_c}{\sigma}\left(\frac{d\ \ln\ m}{dU}\right) \quad (13)$$

where z_+ is the charge on the cation and ν_+ is the number of cations in the dissociated salt (z_- and ν_- are defined similarly for the anion), ϕ_c is the volume fraction of the conducting phase, and F is Faraday's constant.[2,4] We have modified the equation in ref 4 to account for the presence of a nonconducting phase. Combining the measurements shown in Figure 1, one can calculate t_+. The transference number is plotted as a function of salt concentration, r, in Figure 4a. This transference number is a direct function of the mobilities of the cation and anion

$$t_+ = \frac{\mu_+}{\mu_+ + \mu_-} \quad (14)$$

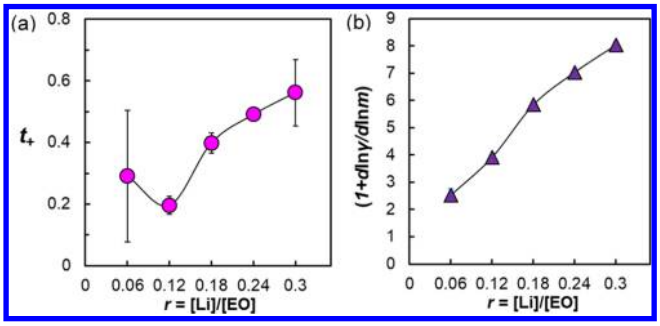

Figure 4. (a) Concentrated solution transference number, t_+, calculated from eq 13 and (b) the thermodynamic factor $1 + \frac{d\ln\gamma}{d\ln m}$ as a function of salt concentration, r, measured at 90 °C.

under the application of an electric field. The overall dependence of t_+ on salt concentration is similar to $t_{+,SS}$ (compare Figures 3c and 4a). If all of the salt molecules in the electrolyte are fully dissociated and the electrolyte is thermodynamically ideal, then $t_+ = t_{+,SS}$;[4] that is, the data in Figures 3c and 4a would overlap. It is clear, however, that this is not the case. Unlike $t_{+,SS}$, which only varies between 0.08 and 0.24, t_+ is much larger and reaches 0.53 at $r = 0.3$. This indicates that the true mobility of lithium ions with respect to the anion is not as low, as indicated by measurements of the steady-state current. The Li and TFSI are equally mobile at the highest salt concentration measured.

DOI: 10.1021/acs.jpcb.7b11371
J. Phys. Chem. B 2018, 122, 1537−1544

The thermodynamic factor, $1 + \frac{d \ln \gamma}{d \ln m}$, is calculated from the concentration potential and the anion transference number, t_-, according to

$$\frac{dU}{d \ln m} = -\frac{v}{z_+ v_+}\frac{RTt_-}{F}\left(1 + \frac{d \ln \gamma_\pm}{d \ln m}\right) \quad (15)$$

where $t_- = 1 - t_+$ and $v = v_+ + v_-$. The thermodynamic factor, calculated using the data in Figures 3d and 4a, is plotted in Figure 4b. At low salt concentrations, this factor approaches unity, the value obtained for ideal solutions, and it increases linearly with salt concentration r. It is not surprising that as more salt is added to the system, the importance of ion−ion and ion−polymer interactions increases and the electrolyte behaves less like an ideal solution.

Stefan−Maxwell diffusion coefficients were calculated from the measured transport coefficients σ, D_m, and t_+ using the following equations

$$\mathcal{D} = \frac{D_m c_0}{c_T\left(1 + \frac{d \ln \gamma_\pm}{d \ln m}\right)} \quad (16)$$

$$\mathcal{D}_{-,0} = \frac{\mathcal{D}}{2t_+} \quad (17)$$

$$\mathcal{D}_{+,0} = \frac{\mathcal{D}}{2(1 - t_+)} \quad (18)$$

$$\mathcal{D}_{+,-} = \left(\frac{c_T F^2 \phi_c}{\sigma RT} - \frac{2c_0 t_+(1 - t_+)}{c_+ \mathcal{D}}\right)^{-1} \quad (19)$$

where $\mathcal{D}$ is the salt diffusion coefficient based on the salt chemical potential, c_0 is the concentration of solvent, $c_T = 2c + c_0$ is the total electrolyte concentration, $\mathcal{D}_{+,0}$ is the Stefan−Maxwell diffusion coefficient describing the interactions between Li and PEO, $\mathcal{D}_{-,0}$ is the Stefan−Maxwell diffusion coefficient describing the interactions between TFSI and PEO, and $\mathcal{D}_{+,-}$ is the Stefan−Maxwell diffusion coefficient describing interactions between Li and TFSI.[2] In the simplest case where the salt dissociates completely, these coefficients describe friction between the ions and solvent, $\mathcal{D}_{+,0}$ and $\mathcal{D}_{-,0}$, and that between the ions, $\mathcal{D}_{+,-}$.

PFG-NMR Characterization and Comparison with Electrochemical Data. Self-diffusion coefficients of lithium- and fluorine-containing species were measured as a function of salt concentration, r, using PFG-NMR. If the salt was fully dissociated, then the PFG-NMR measurements would reflect the motion of individual Li^+ and $TFSI^-$ ions. In Figure 5 we show the fluorine signal attenuation in PEO(5)/LiTFSI and SEO(16−16)/LiTFSI. Extensive studies have shown that in the case of homogeneous polymer electrolytes, the signal attenuation follows single-exponential behavior.[23,35,36] Our measurements of diffusion in PEO(5)/LiTFSI, shown in Figure 5a, are consistent with this. The line through the data represents the best fit of eq 12. In contrast, the signal attenuation in SEO(16−16)/LiTFSI exhibits behavior that is not consistent with a single diffusion coefficient, unlike the measurements of restricted diffusion shown in Figure 2. The curve through the data in Figure 5b, represents the best fit of eq 11 with $D_\parallel$ and $D_\perp$ as adjustable parameters. The presence of two diffusion coefficients is a distinct signature of locally anisotropic diffusion through nanostructured SEO(16−16)/LiTFSI. To our knowledge, no previous studies on characterization of ion transport in block copolymer electrolytes show signatures of anisotropic diffusion.

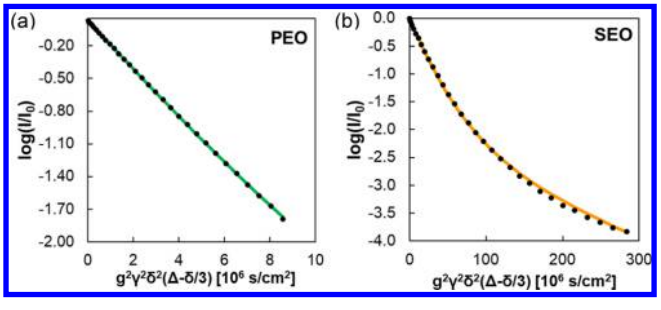

Figure 5. PFG-NMR signal attenuation of ^{19}F seen in (a) PEO(5)/LiTFSI at $r = 0.06$ and (b) SEO(16−16)/LiTFSI at $r = 0.18$.

The dependences of $D_\parallel$ and $D_\perp$ on salt concentration, r, for Li and TFSI are shown in Figure 6. The data sets represent attenuations for different values of δ and Δ, which were adjusted to capture the full decay and to ensure the robustness of $D_\parallel$ and $D_\perp$. It is evident that $D_\parallel$ for both Li and TFSI decreases with increasing r, and $D_\parallel$ of TFSI is faster than that of Li at all values of r. These trends are similar to those obtained for a single isotropic diffusion coefficient in homogeneous PEO/LiTFSI electrolytes.[23] This is expected because $D_\parallel$ represents diffusion within PEO-rich lamellae. At low salt concentrations, $D_\parallel$ of TFSI is much larger than that of Li. In contrast, at high salt concentrations $D_\parallel$ of TFSI is similar to that of Li. This suggests that TFSI dominates ion transport within the lamellae at low salt concentrations, while at high salt concentrations both Li and TFSI contribute more or less equally to ion transport. The increasing importance of lithium transport with increasing salt concentration is reflected in the increase in the transference number shown in Figure 4a. $D_\perp$ is an order of magnitude slower than $D_\parallel$ at low concentrations for both ions, and the two diffusion coefficients approach each other with increasing r.

The Stefan−Maxwell diffusion coefficients calculated using eqs 17 and 18 are also plotted as a function of salt concentration, r, in Figure 6 for Li and TFSI together with the

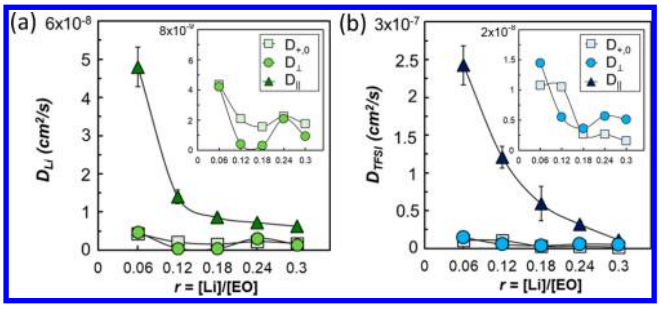

Figure 6. Parallel, $D_\parallel$, and perpendicular, $D_\perp$, diffusion coefficients and the Stefan−Maxwell diffusivities of (a) Li and (b) TFSI in SEO(16−16) as a function of salt concentration, r, at 90 °C.

PFG-NMR diffusion coefficients, $D_\parallel$ and $D_\perp$. The electrochemically determined Stefan−Maxwell diffusion coefficients, $\mathcal{D}_{+,0}$ and $\mathcal{D}_{-,0}$, are in agreement with the diffusion coefficients $D_\perp$ of Li and TFSI determined by PFG-NMR, respectively. The insets in Figure 6 show $\mathcal{D}_{+,0}$, $\mathcal{D}_{-,0}$, and $D_\perp$ for lithium and TFSI on an expanded scale. The agreement between the Stefan−Maxwell diffusivities and $D_\perp$ in Figure 6a,b is nontrivial considering the different approaches used to measure the

DOI: 10.1021/acs.jpcb.7b11371
J. Phys. Chem. B 2018, 122, 1537−1544

diffusivities. This agreement indicates that ion transport through defects strongly influences the electrochemical performance of nanostructured block copolymer electrolytes in batteries.

$\mathcal{D}_{+,-}$, calculated using eq 19 and shown in Figure 7, is negative over the range of salt concentrations studied. A detailed

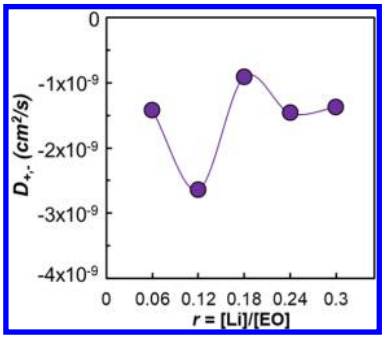

Figure 7. Stefan–Maxwell diffusion coefficient, $\mathcal{D}_{+,-}$, calculated from concentrated solution theory.

explanation of the signs and dependences of the Stefan–Maxwell diffusion coefficients on salt concentration is beyond the scope of this work.

Effect of Morphology on Diffusion. We define a morphology factor

$$f_{\mathrm{NMR}} = \frac{D_{XX} + D_{YY} + D_{ZZ}}{3D_{XX}} \tag{20}$$

where x reflects the preferred direction of ion transport, $D_{XX} \geq D_{YY} \geq D_{ZZ}$. For lamellae pictured in Figure 1, $D_{XX} = D_{YY} = D_{\parallel}$ and $D_{ZZ} = D_{\perp}$. For ideal lamellar and cylindrical samples with $D_{\perp} = 0$, that is, there is no diffusion in the direction orthogonal to the conducting domains, f_{NMR} takes on values of 2/3 and 1/3, respectively. For isotropic samples, f_{NMR} is unity. The dependence of f_{NMR} in SEO(16–16) on r is shown in Figure 8a. These data

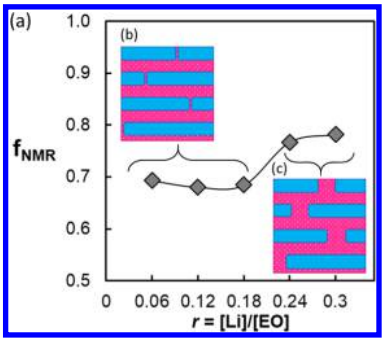

Figure 8. (a) NMR morphology factor, f_{NMR}, calculated from eq 20. Lamellar morphology with (b) small defects and (c) large defects between lamellae.

were obtained by applying eq 20 to Li and TFSI diffusion coefficients and averaging the two results. At low salt concentrations, f_{NMR} is in the vicinity of 2/3, the value expected for ideal lamellae. At high salt concentrations f_{NMR} approaches 0.8. For nonideal morphologies where the neighboring conducting domains are not entirely isolated from each other, we expect f_{NMR} to be larger than the ideal cases.

The local morphology of SEO(16–16) as a function of salt concentration was imaged by transmission electron microscopy (TEM), as shown in Figure 9. Lamellar grains with long internal

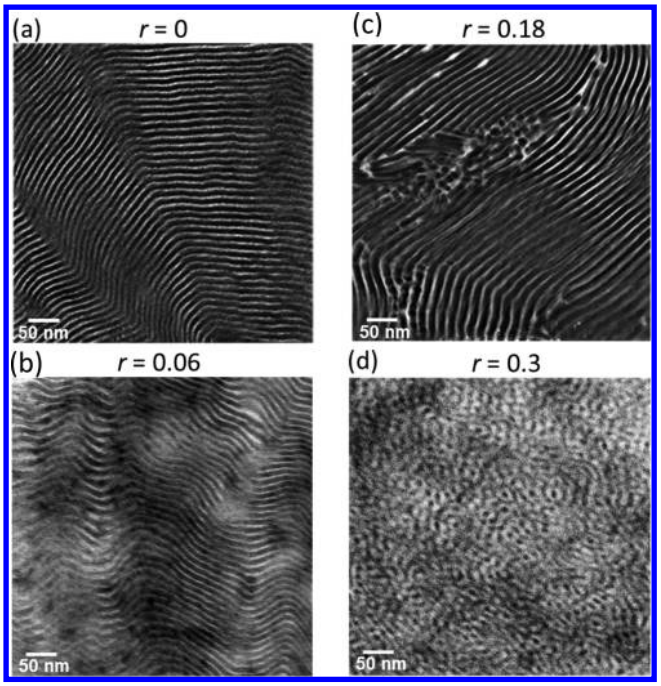

Figure 9. Dark-field transmission electron microscopy images of SEO(16–16) at (a) $r = 0$ and (c) $r = 0.18$, reproduced from Chintapalli et al.[6] and at (b) $r = 0.06$ and (d) $r = 0.3$ measured in this work. The bright phase is poly(ethylene oxide).

order and relatively few defects are evident at $r = 0$, 0.06, and 0.18 in Figure 9a–c. The value of f_{NMR} in this range of r is close to the ideal case. These systems can be described by Figure 8b. At $r = 0.3$ shown in Figure 9d, the lamellar morphology is highly defective. This system is described by Figure 8c, where defects enable ion transport between neighboring lamellar domains and are responsible for the increase in f_{NMR}, seen in Figure 8a.

CONCLUSIONS

We present complete characterization of continuum ion transport in the lamellar block copolymer electrolyte SEO(16–16)/LiTFSI as a function of salt concentration. We report conductivity, mutual salt diffusion, and the electrochemical transference number. Individual diffusion coefficients of the lithium- and TFSI-containing species were measured by PFG-NMR. Fundamental differences between transport of Li and TFSI are seen in both PFG-NMR diffusion and the electrochemically determined transference number. We determine Stefan–Maxwell diffusion coefficients $\mathcal{D}_{+,0}$, $\mathcal{D}_{-,0}$, and $\mathcal{D}_{+,-}$ from the electrochemical measurements and diffusion coefficients parallel to and through defects in the lamellae, $D_{\parallel}$ and $D_{\perp}$ from PFG-NMR. We find that the electrochemically determined Stefan–Maxwell diffusion coefficients, $\mathcal{D}_{+,0}$, and $\mathcal{D}_{-,0}$, fall on top of the diffusion coefficient governing transport through defects in the lamellae, $D_{\perp}$, determined by PFG-NMR. This indicates that transport through defects in an ordered morphology is the limiting factor for electrochemical transport through the bulk. We determine an NMR morphology factor, f_{NMR}, calculated from the anisotropic diffusion tensor. We show that f_{NMR} correlates with defect density seen by TEM.

AUTHOR INFORMATION

Corresponding Authors

*N.P.B.: E-mail: nbalsara@berkeley.edu.

*S.G.G.: E-mail: sgreenba@hunter.cuny.edu.

DOI: 10.1021/acs.jpcb.7b11371
J. Phys. Chem. B 2018, 122, 1537–1544

ORCID

Ksenia Timachova: 0000-0001-8200-3552
Irune Villaluenga: 0000-0002-1299-2479
Mallory Gobet: 0000-0001-9735-0741
Louis A. Madsen: 0000-0003-4588-5183
Nitash P. Balsara: 0000-0002-0106-5565

Author Contributions

#K.T. and I.V. contributed equally to this work. The manuscript was written through contributions of all authors. All authors have given approval to the final version of the manuscript.

Notes

The authors declare no competing financial interest.

■ ACKNOWLEDGMENTS

The work reported here was supported by the National Science Foundation grant NSF-CHE-1333736 in the Designing Materials to Revolutionize and Engineer our Future Program. The NMR work at Hunter College was supported by a grant from the U.S Office of Naval Research.

■ REFERENCES

(1) Hallinan, D. T., Jr.; Balsara, N. P. Polymer Electrolytes. *Annu. Rev. Mater. Res.* **2013**, *43*, 503−525.
(2) Newman, J.; Thomas-Alyea, K. *Electrochemical Systems*; John Wiley & Sons, Inc.: Hoboken, NJ, 2004.
(3) Ma, Y.; Doyle, M.; Fuller, T. F.; Doeff, M. M.; De Jonghe, L. C.; Newman, J. The Measurement of a Complete Set of Transport Properties for a Concentrated Solid Polymer Electrolyte Solution. *J. Electrochem. Soc.* **1995**, *142*, 1859−1868.
(4) Balsara, N. P.; Newman, J. Relationship between Steady-State Current in Symmetric Cells and Transference Number of Electrolytes Comprising Univalent and Multivalent Ions. *J. Electrochem. Soc.* **2015**, *162*, A2720−A2722.
(5) Pesko, D. M.; Timachova, K.; Bhattacharya, R.; Smith, M. C.; Villaluenga, I.; Newman, J.; Balsara, N. P. Negative Transference Numbers in Poly(ethylene Oxide)-Based Electrolytes. *J. Electrochem. Soc.* **2017**, *164*, E3569−E3575.
(6) Chintapalli, M.; Le, T. N. P.; Venkatesan, N. R.; Mackay, N. G.; Rojas, A. A.; Thelen, J. L.; Chen, X. C.; Devaux, D.; Balsara, N. P. Structure and Ionic Conductivity of Polystyrene-Block-Poly(ethylene Oxide) Electrolytes in the High Salt Concentration Limit. *Macromolecules* **2016**, *49*, 1770−1780.
(7) Singh, M.; Odusanya, O.; Wilmes, G. M.; Eitouni, H. B.; Gomez, E. D.; Patel, a J.; Chen, V. L.; Park, M. J.; Fragouli, P.; Iatrou, H.; et al. Effect of Molecular Weight on the Mechanical and Electrical Properties of Block Copolymer Electrolytes. *Macromolecules* **2007**, *40*, 4578−4585.
(8) Mullin, S. A.; Stone, G. M.; Panday, A.; Balsara, N. P. Salt Diffusion Coefficients in Block Copolymer Electrolytes. *J. Electrochem. Soc.* **2011**, *158*, A619.
(9) Bates, C. M.; Chang, A. B.; Momčilović, N.; Jones, S. C.; Grubbs, R. H. ABA Triblock Brush Polymers: Synthesis, Self-Assembly, Conductivity, and Rheological Properties. *Macromolecules* **2015**, *48*, 4967−4973.
(10) Bouchet, R.; Phan, T. N. T.; Beaudoin, E.; Devaux, D.; Davidson, P.; Bertin, D.; Denoyel, R. Charge Transport in Nano-structured PS-PEO-PS Triblock Copolymer Electrolytes. *Macromolecules* **2014**, *47*, 2659−2665.
(11) Young, W. S.; Epps, T. H. Ionic Conductivities of Block Copolymer Electrolytes with Various Conducting Pathways: Sample Preparation and Processing Considerations. *Macromolecules* **2012**, *45*, 4689−4697.
(12) Young, W. S.; Kuan, W. F.; Epps, T. H. Block Copolymer Electrolytes for Rechargeable Lithium Batteries. *J. Polym. Sci., Part B: Polym. Phys.* **2014**, *52*, 1−16.
(13) Zhang, S.; Lee, K. H.; Frisbie, C. D.; Lodge, T. P. Ionic Conductivity, Capacitance, and Viscoelastic Properties of Block Copolymer-Based Ion Gels. *Macromolecules* **2011**, *44*, 940−949.
(14) Panday, A.; Mullin, S.; Gomez, E. D.; Wanakule, N.; Chen, V. L.; Hexemer, A.; Pople, J.; Balsara, N. P. Effect of Molecular Weight and Salt Concentration on Conductivity of Block Copolymer Electrolytes. *Macromolecules* **2009**, *42*, 4632−4637.
(15) Majewski, P. W.; Gopinadhan, M.; Jang, W. S.; Lutkenhaus, J. L.; Osuji, C. O. Anisotropic Ionic Conductivity in Block Copolymer Membranes by Magnetic Field Alignment. *J. Am. Chem. Soc.* **2010**, *132*, 17516−17522.
(16) Gunkel, I.; Thurn-Albrecht, T. Thermodynamic and Structural Changes in Ion-Containing Symmetric Diblock Copolymers: A Small-Angle X-Ray Scattering Study. *Macromolecules* **2012**, *45*, 283−291.
(17) Naidu, S.; Ahn, H.; Gong, J.; Kim, B.; Ryu, D. Y. Phase Behavior and Ionic Conductivity of Lithium Perchlorate-Doped Polystyrene-B-poly(2-Vinylpyridine) Copolymer. *Macromolecules* **2011**, *44*, 6085−6093.
(18) Huynh, T. V.; Messinger, R. J.; Sarou-Kanian, V.; Fayon, F.; Bouchet, R.; Deschamps, M. Restricted Lithium Ion Dynamics in PEO-Based Block Copolymer Electrolytes Measured by High-Field Nuclear Magnetic Resonance Relaxation. *J. Chem. Phys.* **2017**, *147*, 134902.
(19) Ganesan, V.; Pyramitsyn, V.; Bertoni, C.; Shah, M. Mechanisms Underlying Ion Transport in Lamellar Block Copolymer Membranes. *ACS Macro Lett.* **2012**, *1*, 513−518.
(20) Bhattacharja, S.; Smoot, S. W.; Whitmore, D. H. Cation and Anion Diffusion in the Amorphous Phase of the Polymer Electrolyte (PEO)8LiCF3SO3. *Solid State Ionics* **1986**, *18*, 306−314.
(21) Hayamizu, K.; Sugimoto, K.; Akiba, E.; Aihara, Y.; Bando, T.; Price, W. S. An NMR and Ionic Conductivity Study of Ion Dynamics in Liquid Poly (Ethylene Oxide)-Based Electrolytes Doped with LiN(SO2CF3)2. *J. Phys. Chem. B* **2002**, *106*, 547−554.
(22) Gorecki, W.; Jeannin, M.; Belorizky, E.; Roux, C.; Armand, M. Physical Properties of Solid Polymer Electrolyte PEO(LiTFSI) Complexes. *J. Phys.: Condens. Matter* **1995**, *7*, 6823−6832.
(23) Timachova, K.; Watanabe, H.; Balsara, N. P. Effect of Molecular Weight and Salt Concentration on Ion Transport and the Transference Number in Polymer Electrolytes. *Macromolecules* **2015**, *48*, 7882−7888.
(24) Li, J.; Wilmsmeyer, K. G.; Madsen, L. A. Anisotropic Diffusion and Morphology in Perfluorosulfonate Ionomers Investigated by NMR. *Macromolecules* **2009**, *42*, 255−262.
(25) Wang, Z.; Gobet, M.; Sarou-kanian, V.; Massiot, D.; Bessada, C.; Deschamps, M. Lithium Diffusion in Lithium Nitride by Pulsed-Field Gradient NMR. *Phys. Chem. Chem. Phys.* **2012**, *14*, 13535−13538.
(26) Rittig, F.; Kärger, J.; Papadakis, C. M.; Fleischer, G.; Almdal, K.; Štěpánek, P. Self-Diffusion in a Lamellar and Gyroid (Ordered) Diblock Copolymer Investigated Using Pulsed Field Gradient NMR. *Macromolecules* **2001**, *34*, 868−873.
(27) Hamersky, M. W.; Tirrell, M.; Lodge, T. P. Anisotropy of Diffusion in a Lamellar Styrene-Isoprene Block Copolymer. *Langmuir* **1998**, *14*, 6974−6979.
(28) Park, M. J.; Balsara, N. P. Anisotropie Proton Conduction in Aligned Block Copolymer Electrolyte Membranes at Equilibrium with Humid Air. *Macromolecules* **2010**, *43*, 292−298.
(29) Hou, J.; Li, J.; Madsen, L. A. Anisotropy and Transport in Poly(arylene Ether Sulfone) Hydrophilic-Hydrophobic Block Copolymers. *Macromolecules* **2010**, *43*, 347−353.
(30) Patel, S. N.; Javier, A. E.; Stone, G. M.; Mullin, S. a.; Balsara, N. P. Simultaneous Conduction of Electronic Charge and Lithium Ions in Block Copolymers. *ACS Nano* **2012**, *6*, 1589−1600.
(31) Evans, J.; Vincent, C. a.; Bruce, P. G. Electrochemical Measurement of Transference Numbers in Polymer Electrolytes. *Polymer* **1987**, *28*, 2324−2328.
(32) Watanabe, M.; Nagano, S.; Sanui, K.; Ogata, N. Estimation of Li + Transport Number in Polymer Electrolytes by the Combination of Complex Impedance and Potentiostatic Polarization Measurements. *Solid State Ionics* **1988**, *28*−*30* (PART 2), 911−917.

DOI: 10.1021/acs.jpcb.7b11371
J. Phys. Chem. B 2018, 122, 1537−1544

(33) Zibrowius, B.; Caro, J.; Kärger, J. Application of NMR Spectroscopy to Study Diffusion Anisotropy in Polycrystalline Samples. *Z. Phys. Chem.* **1988**, *269O*, 1101−1106.
(34) Tanner, J. E. Use of the Stimulated Echo in NMR Diffusion Studies. *J. Chem. Phys.* **1970**, *52*, 2523−2526.
(35) Hayamizu, K.; Akiba, E.; Bando, T.; Aihara, Y. 1H, 7Li, and 19F Nuclear Magnetic Resonance and Ionic Conductivity Studies for Liquid Electrolytes Composed of Glymes and Polyetheneglycol Dimethyl Ethers of CH3O(CH2CH2O)nCH3 (N = 3 - 50) Doped with LiN(SO2CF3)2. *J. Chem. Phys.* **2002**, *117*, 5929−5939.
(36) Hayamizu, K.; Aihara, Y.; Arai, S.; Martinez, C. G. Pulsed-Gradient Spin-Echo 1H and 19F NMR Ionic Diffusion Coefficient, Viscosity, and Ionic Conductivity of Non-Chloroaluminate Room-Temperature Ionic Liquids. *J. Phys. Chem. B* **1999**, *103*, 519−524.

DOI: 10.1021/acs.jpcb.7b11371
J. Phys. Chem. B 2018, 122, 1537−1544